Line focusing in micro-Raman spectroscopy

M. Ivanda and K. Furić

In a microscope of a micro-Raman spectrometer a cylindrical lens is introduced to form a line-focus microprobe (LFMP). The dimensions of the LFMP are 0.66 × 167 μm. The lateral spatial resolution of Raman scattering with the LFMP is equal to the spatial resolution of the point-focus microprobe (PFMP). It is shown that the LFMP system enables measurements with a laser power density that is 320 times lower than the PFMP. For the same laser power density in both types of illumination, the LFMP Raman spectra give approximately $\sqrt{320}$ or ≈ 18 times better signal-to-noise ratio.

Key words: Micro-Raman spectroscopy, cylindrical lens, microscopy, spectroscopic techniques.

1. Introduction

In 1974, and 1975 Rosasco *et al.*[1,2] and Delhaye and Dhamelincourt[3] showed that laser-excited Raman scattering could be extended to the analysis of micrometer- and submicrometer-sized particles by using a microscope objective in the sampling scheme. In the past few years there have been significant developments in the micro-Raman spectroscopic technique, and nowadays it is an established tool in the laboratory.[4–9] It is also used in concert with other instrumental microanalysis techniques and, in general, a combination of such studies is most successful approach.

Heating and photoinduced processes[4] represent big problems in Raman microanalysis because of subsequent physical and chemical modifications of the sample resulting from the absorption of the focused laser light. Macro-Raman spectroscopy avoids these problems by using fast relative motion between the sample and the incident laser beam[10,11] or by introducing a cylindrical lens (CL) in the 45° and 90° scattering geometry.[12] The basic idea of the last modification is to change the illuminated area of the sample so that it approaches slit geometry and makes it possible to collect the maximum amount of scattered light at a minimum laser irradiation.

Here a new optical design for the formation of the line-focus microprobe (LFMP) by the CL in micro-Raman spectroscopy is presented. Other line-focus geometries in Raman microanalysis have been reported by Bowden *et al.*[13] and Delhaye and Dhamelincourt.[3] The optical system discussed in this paper does not preserve information about the spatial distribution along the line focus, but permits easy transition of the spectrometer configuration from the point-focus microprobe (PFMP) to the LFMP by inserting an appropriate CL in the tube of a microscope. The results are illustrated by comparison of the Raman spectra of silicon recorded in the two laser focus geometries.

2. Line Focusing by Microscope

Figure 1 presents a diagram of the laser light rays in an optical system that consists of a CL and a spherical lens (SL). Table 1 lists the symbols and values of all relevant optical parameters used in the figures, equations and text. The CL forms a line focus that is the object for the SL. The length of the line focus is equal to the diameter of the incident laser beam. The SL forms a primary and a secondary image. The length of the primary image can be calculated by the standard lens formula. The secondary image is formed at the light-ray intersection in the focal plane of the SL. In the approximation of a parallel incident laser beam, the distance of the secondary image from the SL is equal to the focal length of the SL, and its length is given by

$$L = \frac{f_{ob}}{f_c} d. \tag{1}$$

In the present experiment an infinity-corrected LBM Olympus microscope objective (MO) is used at the position of the SL shown in Fig. 1. It forms a parallel beam of light from a point source in the focal plane of the MO. If the diameter of the beam on the MO is larger than the aperture of the MO, d in Eq. (1)

The authors are with the Ruder Bošković Institute, P.O. Box 1016, 41000 Zagreb, Bijenička 54, Croatia.

Received 20 May 1991.
0003-6935/92/306371-05$05.00/0.

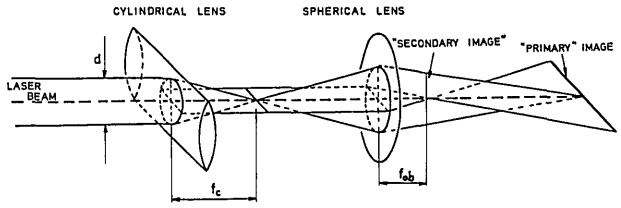

Fig. 1. Paths of laser light rays in an optical system that consists of a CL and a SL. The symbols used are defined in Table 1.

must be replaced by the effective laser beam diameter

$$d_{\text{eff}} = \frac{f_c}{l_{\text{co}} - f_c} d_{\text{ap}}. \tag{2}$$

Figure 2 shows the optical design of the micro-Raman spectrometer modified for line focusing. The modification was easily done by inserting a CL in the tube of the microscope. According to Fig. 1 the secondary image is formed in the focal plane of the MO. It is used as the LFMP Raman excitation. The CL orientation enables the secondary image line focus to be collinear with the spectrometer slit. In the approximation of the uniform irradiance over the objective aperture, half of the width of the LFMP is equal to the Airy disk radius[4]:

$$r = \frac{0.61\lambda}{\text{NA}}. \tag{3}$$

The CL forms a real image inside the tube of the microscope from the scattered light collected by the objective. This image is the object for the optical

Table 1. Definitions of Symbols and Values Used

Symbol	Value	Definition
f_c	45 mm	Focal length of CL
f_{ob}	2.5 mm	Focal length of 100× microscope objective (MO)
f_1	95 mm	Focal length of lens L_1
f_2^r	250 mm	Focal length of right focus of system of lenses L_2
f_2^l	140 mm	Focal length of left focus of system of lenses L_2
f_3	200 mm	Focal length of lens L_3
f_4	80 mm	Focal length of lens L_4
l_{co}	90 mm	Distance between CL and MO
	20 mm	Distance between point P and lens L_3
	410 mm	Distance between lens L_3 and lens L_4
d_{ap}	3 mm	Diameter of aperture of 100× MO
d	6 mm	Diameter of incident laser beam at CL
h	18 mm	Height of spectrometer slit
w	>100 μm	Width of spectrometer slit
M_{ob}	100	Magnification of MO
M_S	0.23	Magnification of system of lenses outside the microscope
L	167 μm	Length of LFMP at focal plane of MO
NA	0.95	Numerical aperture of 100× MO
f_s	10	f-number of spectrometer
n	1	Index of refraction of medium between sample and front lens of microscope

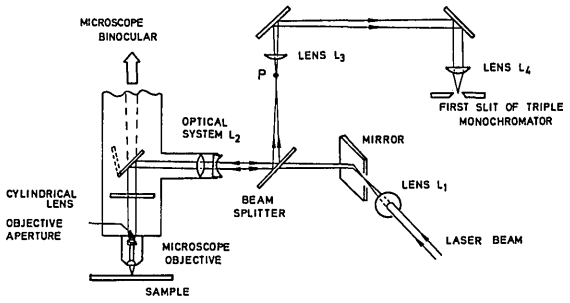

Fig. 2. Raman microscope with CL inserted for laser line focusing. Laser epi-illumination of the sample is used.

system L_2. Without the CL present, the optical system L_2 of the microscope is designed in such a way that the magnification at point P (which is the right focal point of the system of lenses L_2) is equal to the magnification of the MO. With the CL present, the analysis of the image at point P is the following: if we assume that the microscope is focused on the secondary image and is well corrected for infinity (which is the case for infinity-corrected MO), then each is on the right focal plane of the system of lenses L_2, and the length of the secondary source image L_P is given by Eq. (1) with f_{ob} replaced by f_2^r and d replaced by d_{ap}, i.e., $L_P = (f_2^r/f_c) * d_{ap}$. This would effectively lengthen the image produced by the MO, $M_{ob}L$, additively by the length L_P. Therefore the magnification of the system at point P in the direction parallel to the entrance slit of the spectrometer is given by

$$M_{P\parallel} = M_{ob} + \frac{f_2^r d_{ap}}{f_c L}. \tag{4}$$

The magnification at point P in the direction normal to the entrance slit is not affected by the CL, i.e., $M_{P\perp} = M_{ob}$. If the distance from the main plane of the left focus of the optical system L_2 to the CL is higher from the sum of the focal length f_2^l and f_c, the rays of the scattered light beyond the secondary image at point P would be convergent. The magnification at the first slit of the triple monochromator for the two directions (normal and parallel to the slit) can be written as

$$M_{\perp,\parallel} = M_{P\perp,P\parallel} * M_S \tag{5}$$

The magnification of the system of lenses L_3 and L_4, M_S, is arranged for the maximal light collection efficiency and full spectrometer resolution in the PFMP configuration. Because the magnification $M_{P\perp}$ is not affected by the CL, the same arrangement is valid for the $M_\perp$ in the LFMP configuration. Consequently $M_\perp$ should be[14]

$$M_\perp = (\Omega_{ob}/\Omega_s)^{1/2}, \tag{6}$$

where Ω_{ob} and Ω_s are solid angles of the MO and of the collecting mirror of the spectrometer monochromator, respectively. Therefore, the magnification M_S

should be

$$M_S = (\Omega_{ob}/\Omega_s)^{1/2}/M_{P\perp}. \quad (7)$$

Consequently, the width of the LFMP under the MO should not exceed the value $D_{max} = w/M_\perp$. Considering the geometrical parameters of the scattered light collection, we find that the solid angles are

$$\Omega_{ob} = 2\pi[1 - [1 - (NA/n)^2]^{1/2}], \quad (8)$$

$$\Omega_s = 2\pi[1 - [1 + (2f_S)^{-2}]^{-1/2}]. \quad (9)$$

The magnification in the direction that is parallel to the entrance slit, $M_\parallel$, must be considered only for the optimal coupling of the length of the LFMP to the slit height. Therefore the length of the LFMP should not exceed the value $L_{max} = h/M_\parallel$.

In the current study the MO used had the following parameters: 100× magnification, NA = 0.95, and $f_{ob} = 2.5$ mm. According to the value obtained from Eq. (7), the system of lenses L_3 and L_4 is designed for the magnification $M_S = 0.235$. Therefore the maximal allowed dimensions of the LFMP are $L_{max} = 383$ μm and $D_{max} = 4.3$ μm (for the slit width $w = 100$ μm). To provide the approximation of the uniform irradiance over the whole aperture, the diameter of the laser beam inside the tube of the microscope was chosen to be approximately 2 times larger than the aperture of the MO. The distance of the CL from the MO was chosen as $l_{co} = 2f_c$; therefore, according to Eq. (2), the effective laser beam diameter on the MO was equal to d_{ap}. The dimensions of the LFMP, as calculated by Eqs. (1) and (3), are $L = 167$ μm and $D = 0.66$ μm, which are the lower than maximal values allowed. In this way, the total light of the image formed at the entrance slit is transferred to the monochromator.

3. Comparison of Light Scattering with LFMP and PFMP excitation

In order to compare the efficiency of the LFMP with that of the PFMP in the scattering experiment we used Raman spectra recorded on the silicon (111) plane and illuminated by a focused linear polarized light from a Coherent INNOVA 100 argon-ion laser at λ = 514.5 nm. Raman spectra were recorded with a Dilor Z-24 Raman spectrometer equipped with an Olympus BH microscope for micro-Raman spectroscopic measurements.

Large laser power density on the silicon raises the local temperature and increases the concentration of the free carriers. The effect of the free carriers on the optical phonons of silicon at the zone center [$TO(\Gamma)$] is well documented.[15,16] The quantum interference between discrete (one-phonon) with continuum (intervalence-band) states results in a Fano scattering line that is asymmetric, broadened, and shifted to lower frequencies. An increase in the temperature has similar effects.[17] Therefore the frequency downshift and the line broadening of the silicon $TO(\Gamma)$ band can be a measure of the influence of the laser irradiation.

The comparison of some parameters of the silicon phonon band versus laser power on the sample in the case of the PFMP and LFMP optical configuration is given in Fig. 3: the variation of the peak position [Fig. 3(a)], the FWHM [Fig. 3(b)], and the integral intensity [Fig. 3(c)]. The PFMP has 320 times higher a laser power density that is than the LFMP. It follows that even a relatively low laser power at the sample (15 mW) in the PFMP configuration affects the peak position and FWHM of the phonon band. On the other hand, the LFMP has a low influence on the same band; only a 0.3-cm^{-1} frequency shift and a 0.4-cm^{-1} line broadening in the whole laser power interval is observed. The integral intensity is linear with applied laser power and approximately equal in both cases up to 70 mW, which shows that the addition of the CL in the microscope has no effect on the throughput of the collection optics. For a laser power higher than 70 mW, the signal intensity obtained with the PFMP increases faster, which may be

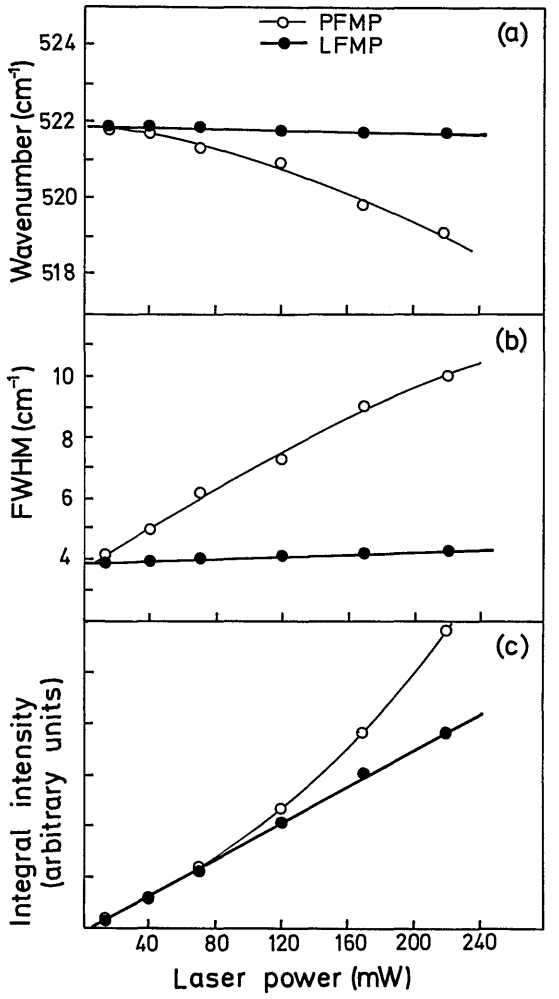

Fig. 3. (a) Wave number, (b) FWHM, and (c) integral intensity of a silicon $TO(\Gamma)$ phonon band in Raman spectra taken with the PFMP and the LFMP excitation as a function of the laser power at the sample.

due to additional light scattering because of the Fano-type resonance.[15,16]

The Raman spectra for the points of the lowest and the highest laser power in the sample from Fig. 3 are shown in Fig. 4. With a 15-mW laser power [Fig. 4(a)], the intensities of the bands are approximately equal. A slight signal lowering, which was observed in the case of the LFMP configuration, can be attributed to the losses of the scattered light in a transmission through the added CL. With a 220-mW laser power [Fig. 4(b)], the difference between the phonon bands obtained with the two illuminations considered is evident.

Figure 5(a) shows the Raman spectrum obtained in the PFMP configuration with $P_1 = 0.69$ mW laser power at the sample. Figure 5(b) shows a Raman spectrum obtained with the LFMP and $P_2 = 220$ mW laser power at the sample. Nevertheless, the laser power density at the sample in both cases is equal (≈ 200 kW/cm^2). Because of the higher laser power in the LFMP case, a signal intensity that is 320 times higher is expected, which agrees well with the observed values shown in Fig. 5. At the same time, the signal-to-noise ratio for the LFMP configuration can be expected to be improved on the basis of the simple relation $\sqrt{P_2/P_1} = \sqrt{320} \approx 18$ [see Eq. (4), Ref. 18]. The measured value was usually slightly different, especially at the level of light signals that were close to the threshold of the detectability. This fact can be attributed to the observed imperfections of the photon counting detection chain used in this experiment.

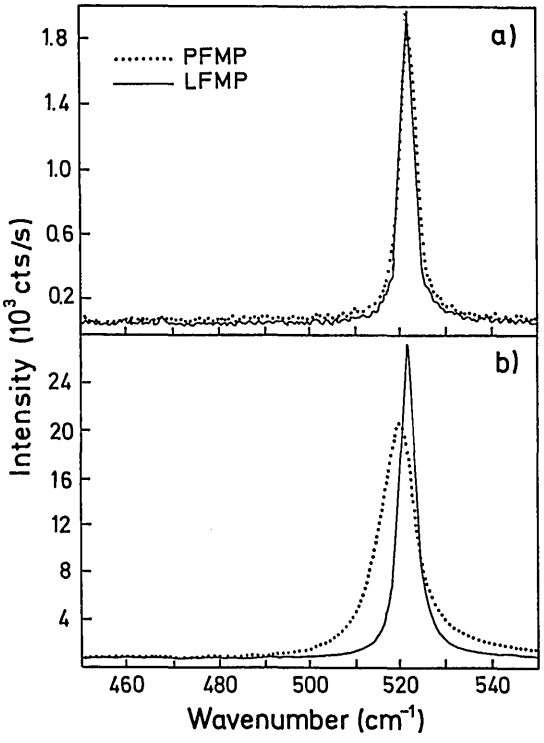

Fig. 4. Raman spectra of a silicon $TO(\Gamma)$ phonon band taken with the PFMP and the LFMP excitation. Laser powers at the sample are (a) 15 mW, (b) 220 mW; slit width, 300 μm; scanning step, 0.5 cm^{-1}; accumulation time, 1 s.

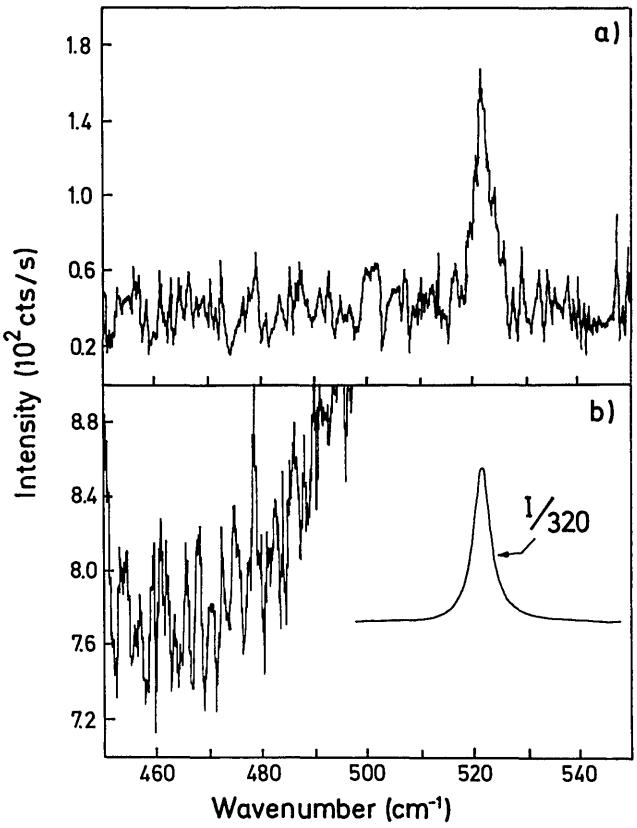

Fig. 5. Raman spectra of a silicon $TO(\Gamma)$ phonon band taken with ≈ 200 kW/cm^2 of laser power density at the sample: (a) PFMP excitation, (b) LFMP excitation. Slit width, 300 μm; scanning step, 0.5 cm^{-1}; accumulation time, 1 s.

To show another example of possibilities offered by the micro-Raman spectrometer completed with the LFMP we have taken a spectrum of amorphous silicon. Generally, the Raman signal intensity of amorphous silicon is relatively low. To avoid laser-induced crystallization, low laser irradiation of the sample must be used. Therefore, even in the macro-Raman spectroscopy, the CL in quasi-backscattering geometry is often used. Figure 6 shows a relatively good Raman spectrum of amorphous silicon that was

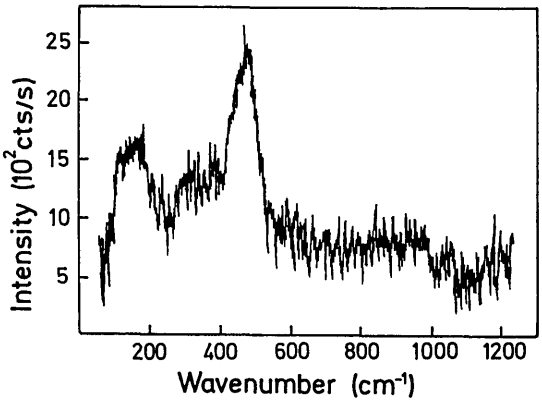

Fig. 6. Raman spectrum of amorphous silicon taken with the LFMP excitation. Laser power at the sample, 220 mW; Slit width, 800 μm; scanning step, 3 cm^{-1}; accumulation time, 3 s.

obtained with the LFMP excitation. This shows the possibility of an LFMP modification for recording of weak scatterers and samples that are sensitive to temperature and photoinduced changes.

The optical system discussed in this paper does not preserve information about the spatial distribution along the line focus (irrespective of the detector) and thus appears to be useful mainly to systems in which information with a spatial resolution element of $0.66 \times 167\ \mu m^2$ is interesting. Therefore it can be applied in laser spectroscopy measurements (Raman, photoluminescence, etc.) of thin-layered structures and in laser material processing.

The authors are grateful to L. Colombo for valuable discussions during the preparation of the manuscript.

References

1. G. J. Rosasco, E. S. Etz, and W. A. Cassatt, "Investigation of Raman spectra of individual micrometer-size particles," presented at the Fourth International Conference on Raman Spectroscopy, Brunswick, Maine, August 1974.
2. G. J. Rosasco, E. S. Etz, and W. A. Cassatt, "The analysis of discrete fine particles by Raman spectroscopy," Appl. Spectrosc. **29,** 396–404 (1975).
3. M. Delhaye and P. Dhamelincourt, "Raman microprobe and microscope with laser excitation," J. Raman Spectrosc. **3,** 33–43 (1975).
4. G. J. Rosasco, "Raman microprobe spectroscopy" in *Advances in Infrared and Raman Spectroscopy,* R. J. H. Clark and R. E. Hester, eds. (Heyden, New York, 1980), Vol. 7, pp. 223–282.
5. P. M. Fauchet, "The Raman microprobe: a quantitative analytical tool to characterize laser-processed semiconductors," IEEE Circuits Devices Mag. **2,** 37–53 (1986).
6. R. K. Janssen and D. M. Krol, "Micro-Raman spectroscopy: a technique for analyzing bubbles in glass," Appl. Opt. **24,** 275–279 (1985).
7. H. Morishita, T. Ishida, M. Kobayashi, and K. Sato, "Study of micropolytype structures in crystals of steraic acid B form by the Raman microprobe technique," J. Phys. Chem. **91,** 2273–2278 (1987).
8. B. Wopenka and J. D. Pasreris, "Limitations to quantitative analysis of fluid inclusions in geological samples by laser Raman microprobe spectroscopy," Appl. Spectrosc. **40,** 144–151 (1986).
9. C. Ballan-Dufrancais, M. Truchet, and P. Dhamelincourt, "Interest of Raman laser microprobe (MOLE) for the identification of purinic concretions in histological sections," Biol. Cellulaire **36,** 51–58 (1979).
10. W. Keifer, "New Raman techniques," in the Fourth International Conference on Raman Spectroscopy, Brunswick, Maine, August 1974.
11. W. Keifer, "Recent techniques in Raman spectroscopy" in *Advances in Infrared and Raman Spectroscopy,* R. J. H. Clark and R. E. Hester, eds. (Heyden, New York, 1977), Vol. 3, pp. 1–42.
12. H. H. Eysel and S. Sunder, "Line focus method for recording laser Raman spectra of colored solids," Appl. Spectrosc. **34,** 89–90 (1980).
13. M. Bowden, D. J. Gardiner, and G. Rice, "Line-scanned micro-Raman spectroscopy using a cooled CCD imaging detector," J. Raman Spectrosc. **21,** 37–41 (1990).
14. M. Hercher, W. Mueller, S. Klainer, R. F. Adamowicz, R. E. Meyers, and S. E. Schwartz, "An efficient intracavity laser Raman spectrometer," Appl. Spectrosc. **32,** 298–302 (1978).
15. F. Cerdeira and M. Cardona, "Effect of carrier concentration on the Raman frequencies of Si and Ge," Phys. Rev. B **5,** 1440–1454 (1972).
16. F. Cerdeira, T. A. Fjeldly, and M. Cardona, "Effect of free carriers on zone-center vibrational modes in heavily doped *p*-type Si. II. Optical modes," Phys. Rev. B **8,** 4734–4745 (1973).
17. T. R. Hart, R. L. Aggarwal, and B. Lax, "Temperature dependence of Raman scattering in silicon," Phys. Rev. B **1,** 638–642 (1970).
18. J. J. Freeman, J. Heaviside, P. J. Hendra, J. Prior, and E. S. Reid, "Raman spectrometry with high sensitivity," Appl. Spectrosc. **35,** 196–202 (1981).